HARDMEKO 2007
Recent Advancement of Theory and Practice in Hardness Measurement
19-21 November, 2007, Tsukuba, Japan

APPLICATION OF INDENTATION TEST TO THE EVALUATION OF TBC YOUNG'S MODULUS

Motofumi OHKI[1], *Tatsuya ISHIBASHI*[1], *Jun KINOSHITA*[2] *and Hiroki UCHIYAMA*[2]

[1] Faculty of Engineering, Niigata University, Niigata, Japan
[2] Graduate School of Science and Technology, Niigata University, Niigata, Japan

Abstract – Thermal barrier coatings (TBCs) have been applied to vanes / blades of gas turbines for recent electric power stations and these contribute to the efficiency of gas turbines. Measurement of Young's modulus of the top-coat of TBCs with high accuracy is important since it is a dominant factor for determining the magnitude of thermal stress. However, until now, evaluation method for Young's modulus of the top-coat has not been established, due to difficulty of material testing in its coated form. Furthermore, a porosity of the top-coat is changed by progress of sintering phenomenon caused by long-term high temperature exposure in air, consequently Young's modulus of the top-coat is also influenced.

In this study, various trials to evaluate Young's modulus of the top-coat for application of the indentation test were conducted. Firstly, both dependency of the testing load and anisotropy on calculated Young's modulus of the top-coat were discussed. Next, measurement of Young's modulus of the top-coat after long-term high temperature exposure was carried out. Obtained results were verified by comparing with other method to measure Young's modulus of the top-coat.

Keywords: Thermal barrier Coatings, Young's modulus of top-coat, Indentation test

1. INTRODUCTION

In view of the terrestrial environment and energy consumption, operation gas temperature elevation of gas turbines for electric power stations is required. As the key technology to achieve this, adding Thermal Barrier Coatings (TBCs) to blade metallic components has been a common procedure. Generally, TBCs consist of under-coat (UC) and top-coat (TC). UC (usually MCrAlY alloy is selected) prevents both oxidation and erosion of metallic substrate, and also maintains adhesion between TC and substrate. TC (usually a low thermal conductivity ceramic is selected) has a thermal barrier property. By combining with TBCs and internal blade cooling, substrate temperature becomes about 100ºC lower and operation gas temperature can be elevated [1].

On the other hand, the repetition of thermal stress caused by difference in the thermal expansion coefficient between ceramic TC and metallic UC / substrate promotes coating damage [2]. Therefore, understanding the accurate value of TC Young's modulus that can estimate the extent of generated thermal stress is necessary to ensure material reliability. However, because TBCs are formed as a composite material of combined thin layer coatings, the essential problem that TBCs can't apply to general materials estimation experiment is obvious. Furthermore, during long-term high temperature exposure, occurrence of TC densification (decreasing TC porosity) which changes TC Young's modulus with comparison of its initial modulus is also reported [3]. Therefore, simple, quick, accurate, and non-destructive measurement of TC Young's modulus is needed, but such measurement is not established yet.

The indentation hardness test is one of non-destructive material tests. It is studied by a number of researchers including us over wide range from theoretical discussion of the indentation process [4] to practical application [5]. Recently, nanoindentation measuring the indentation load and displacement during the indentation process for a very low load level has been developed. It can estimate some material properties that can't be estimated by conventional hardness tests, such as Young's modulus and yield stress. As it also can test simply and quickly, it seems appropriate for the method of TC Young's modulus measurement.

In this study, application of the indentation test to evaluate TBC Young's modulus was carried out. First, the suitable testing load was examined on a load range from 4.9 to 441 N. In other words, it is dependency of the testing load on calculated Young's modulus of TC. From the results, significant load dependency on calculated Young's modulus was shown. The investigation by the finite element method of indentation and the analysis of acoustic emission signals showed that the dependency is caused either by a correlation between indentation depth and the thickness of TC layer, or crushed damages of TC around the indentation.

Second, influences of indentation directions on the calculated Young's modulus of TC were discussed. This topic is equivalent to anisotoropy on calculated Young's modulus of TC. From the result, it was found that the Young's modulus of TC calculated by means of this research indicates less anisotoropy.

Finally, measurement of Young's modulus of TC after long-term high temperature exposure was conducted. Obtained results were compared with the results of Young's modulus calculated by the other procedure, based on the

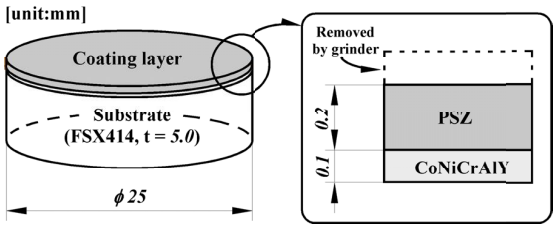

(a) TBC specimen.

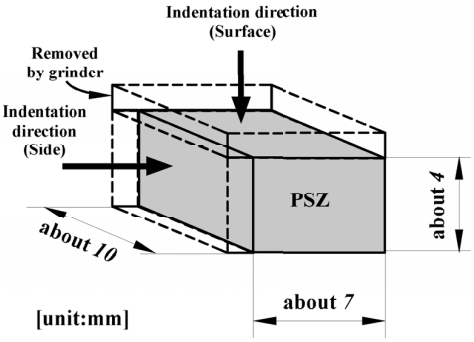

(b) Top-coat (TC) specimen.

Fig. 1 Geometry and shape of specimens used in this study.

relationships between TC porosity and Young's modulus. From these investigations, validity of both evaluation methods was discussed.

2. EXPERIMENTAL PROCEDURES

2.1. Specimens

Two kinds of specimens were prepared to discuss the influence of load dependency and TC anisotropy on calculated TC Young's modulus. Fig. 1(a) shows the geometry and shape of general TBC specimen used in the discussion about the influence of load dependency (after this, this specimen is referred to as a TBC specimen). In this specimen, Co-base super alloy FSX414 was used as substrate, CoNiCrAlY alloy as UC and 7wt%Y_2O_3 partially stabilized ZrO_2 (PSZ) as TC. The chemical composition of each element used in the specimen is shown in Table 1. Since as-sprayed specimens had some surface roughness caused by random deposition of splats, we ground specimen surface about 0.1 mm to avoid the effect of surface roughness.

We also prepared free-standing top-coat specimens that were sprayed thickly until there was about 5 mm on the substrate. Then the substrate was removed chemically (after this, this specimen is referred to as a TC specimen). Both top and side surfaces of such TC specimen were ground, and then indentation tests were carried out on each surface. Fig. 1(b) shows the geometry and shape of a TC specimen. The chemical composition and spray condition were the same as the TBC specimen.

To discuss the influence of long-term high-temperature exposure to Young's modulus of TC, a TBC specimen was subjected the long-term high temperature exposure (air environment, 900ºC, and 1 year) by using an electric furnace.

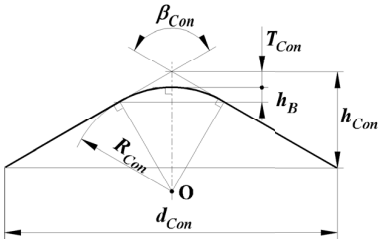

Fig. 2 Schematic illustration of truncated conical indenter.

2.2. Indentation tester

In this study, a mechanically-driving indentation tester developed in our laboratory was used as a testing apparatus. The spectacle shape component (material: brass for low loads and steel for high loads) with sticking strain gages was used as the load-cell. The bridge circuit was constructed with a bridge box and the load-cell, and this circuit was connected to the strain amplifier (Shinkoh DAS-406). As displacement measurement instruments, we used a linear proximity sensor (OMRON E2CA-X1R5A) with an amplifier unit (E2CA-AN4C). The resolution of this system was 0.6 μm. To calibrate the inclination of the specimen table, four sensors were equipped at the ends of the specimen table, and displacement data from them were averaged. Indentation load and displacement data were inputted in a personal computer (PC) via an analog / digital transformer board inserted in the PC slot. The PC also controlled the tester movement. Other features of the tester were that the indenter was driven by mechanical elements with high reliability (stepping motor and ball screw, minimum displacement: 40 nm), and various types of indenters such as pyramidal, conical, and spherical, could be applied by using the holder.

2.3. Indentation conditions (Load and Indenter)

Indentation tests were carried out five times at all following indentation loads; 4.9, 9.8, 29.4, 49, 98, 147 N (in addition, indentation tests of 294 N were also carried out to discuss the influence of load dependency on calculated TC Young's modulus).

About indenter shape, another researcher reported that the results of indentation for TC, which has a porous body, were influenced by the indenter shape [6]. Namely, these were the results of indentation with a pyramidal indenter reflecting the property of a relatively small area. However, indentations with a conical or a spherical indenter, which has a relatively wide contact area compared with a pyramidal indenter, reflect the average property of a certain amount of area. The calculated TC Young's modulus discussed in this study means Young's modulus obtained from whole TC as an accumulated body of PSZ particles, and not Young's modulus obtained from only PSZ particle. Therefore, it seems that a conical (or spherical) indenter is appropriate to use for such purposes. Then we chose a conical indenter for the Rockwell hardness test. Fig. 2 indicates the indenter tip shape of a conical indenter. This indenter regulated tip angle β_{Con} and tip curvature radius R_{Con} (tip angle β_{Con} =119°55', tip curvature radius R_{Con} =195

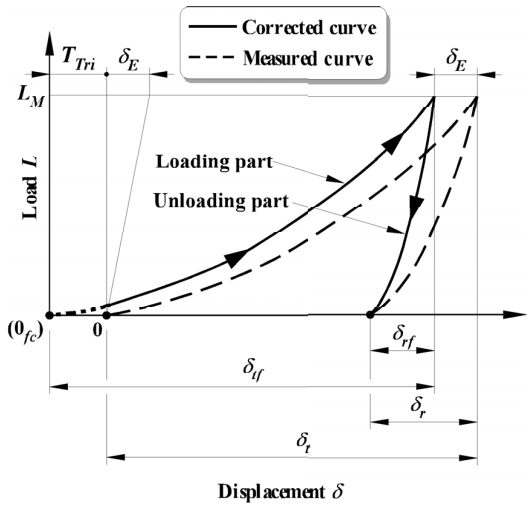

Fig. 3 Schematic illustration of relationships between indentation load and displacement.

μm), so the truncation of tip T_{Con} (difference between indenter height for ideal shape h_{Con} and that for practical shape having a tip curvature radius) was geometrically obtained, and it is shown in (1).

$$T_{Con} = R_{Con}\left\{\frac{1}{\sin(\beta_{Con}/2)} - 1\right\} \tag{1}$$

Then, the relationship between the diameter of indenter bottom d_{Con} and the indenter height for ideal shape h_{Con} is expressed in (2).

$$d_{Con} = 2 \cdot h_{Con} \cdot \tan\left(\frac{\beta_{Con}}{2}\right) \tag{2}$$

2.4. Acoustic emission (AE) sensor

To discuss the influence of load dependency on calculated TC Young's modulus, an acoustic emission (AE) sensor (AE901S, made by NF Corp.) was equipped on the indentation surface of the specimen and connected to an AE tester (No. 9501, made by NF Corp.). AE output data was inputted into the PC, which also had the indentation load and displacement data input. By combining AE and indentation data, we could discuss the correlation between the indentation process and behaviour of materials deformation and fractures.

2.5. Calculation theory of Young's modulus

In this study, TC Young's modulus was measured by using the calculation theory of Young's modulus with a conical indenter proposed by Amano et.al. [7-8]. Schematic illustration of the indentation load-displacement curve obtained from the indentation test is shown in Fig. 3. This figure suggests that it is necessary to consider the effect of the elastic deformation of the tester itself and the truncation of indenter's tip. Thus, the true indentation depth δ_{tf} (= $\delta_t - \delta_E + T_{Con}$) and the true elastic recovery δ_{rf} (= $\delta_r - \delta_E$) can be obtained.

From Hertz's elastic contact theory [9], the relationship of the indentation load L_M, the contact diameter between the indenter and specimen surface d_C, the true elastic recovery

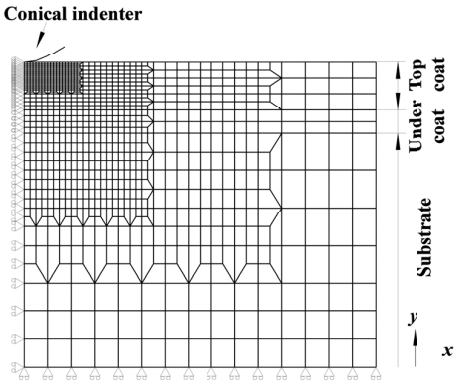

Fig. 4 Schematic illustration of FEM analysis model.

δ_{rf} and the elastic parameter between indenter and specimen $F(E)_{IS}$ is expressed in (3).

$$L_M = \left(\frac{2}{3}\right)\frac{d_C \cdot \delta_{rf}}{F(E)_{IS}} \tag{3}$$

$F(E)_{IS}$ is also expressed in (4).

$$F(E)_{IS} = \frac{1-\mu_I{}^2}{E_I} + \frac{1-\mu_S{}^2}{E_S} = I(E) + S(E) \tag{4}$$

Here, μ_I: Poison's ratio of the indenter (= 0.07), E_I: Young's modulus of the indenter (= 1140 GPa), μ_S: Poison's ratio of the specimen, E_S: Young's modulus of the specimen, $I(E)$: the elastic parameter of the indenter, $S(E)$: the elastic parameter of the specimen.

In (2), d_{Con} is replaced by d_C, and h_{Con} is also replaced by δ_{tf}. Then (2) and (4) are substituted for (3). Finally, by rearrangement, calculation formula for Young's modulus of the specimen $E_{S(i)}$ can be obtained.

$$E_{S(i)} = \left(1-\mu_I{}^2\right) \Big/ \left[\left(\frac{4}{3\sqrt{\pi}}\right)\frac{K_{0(Con)} \cdot \delta_{tf} \cdot \delta_{rf}}{L_M} - I(E)\right] \tag{5}$$

The elastic deformation of tester δ_E is obtained by using (5) and practical test data recorded on HV500, which is the standard block for hardness tests and the specimen for calibration in this study because its properties are known (especially Young's modulus = 210 GPa).

2.6. Finite Element Method (FEM) stress analysis

To discuss the distribution of strain in material during indentation, we carried out stress analysis with general Finite Element Method (FEM) analysis code MSC. Marc. The finite element model used in the present study is shown in Fig. 4. The element type was a two dimensional axisymmetric type with eight nodes, and the indenter was regarded as a rigid body. As boundary conditions, the nodes on the symmetric axis (in this analysis, x-axis was regarded as the symmetric axis) were restricted for horizontal displacement and nodes on the bottom surface were restricted for vertical displacement. To simplify the modelling of the indentation analysis on the TBC specimen surface using a conical indenter, it is regarded as elastic analysis. The analyzed area is limited until both 1 mm radius and 1.3mm depth from indentation centre.

The critical condition to finish analysis is to reach an indenter displacement of 8 or 20 μm in 10 steps.

2.7. Measurement of TC porosity

To discuss the influence of porosity change to calculated Young's modulus of TC, two dimensional porosity of TC was measured from cross-sectional TC images and image treatment application. Then, following (6) was used to calculate Young's modulus from porosity,

$$E_{S(P)} = E_0 \cdot \exp(-bP) \quad (6)$$

where E_0: Young's modulus without pore, P: porosity, b: material constant. From reference values (41 GPa and 18.3 %), b was obtained as 8.66.

3. RESULTS AND DISCUSSION

3.1. Influence of load dependency

Relationship between indentation load and calculated Young's modulus of TC is shown in Fig. 5. This result suggested the presence of load dependency on calculated Young's modulus of TC.

Relationships between indentation load, AE rate, and displacement at indentation load 294 N on the TBC specimen are shown in Fig. 6 (figures at other loads are omitted due to limitations of space). From these results, the load-displacement curve was smooth and very few AE signals were generated up to 147 N, but irregular behaviour of the load-displacement curve and significant generation of the AE signals were recorded from 294 N. It is generally known that AE signals are generated from movements of dislocation with slip and twin [10]. AE signals of indentation loads at 147 N were almost at noise level, but sometimes meaningful signals were generated, especially in the region of maximum load at 147 N. Such sporadic signals correspond to signals generated by plastic deformation mentioned above. On the other hand, AE signals generation behaviour of indentation load at 294 N was quite difference with its signal intensity compared with lower load. Therefore, significant generation of AE signals on indentation load from 294 N wasn't caused by plastic deformation, and the reason for the decrease in TC Young's modulus with an increasing indentation load above 147 N is displacement promotion such as the pop-in phenomenon [11] caused by TC fracture.

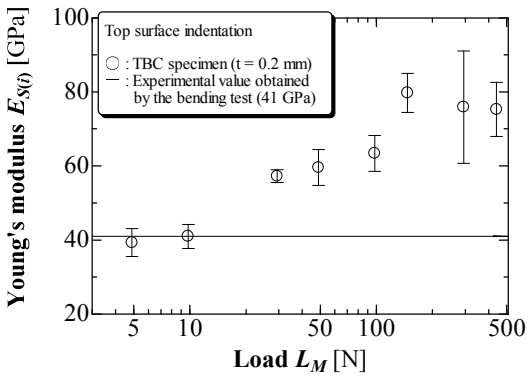

Fig. 5 Relationship between indentation load and calculated Young's modulus of TC

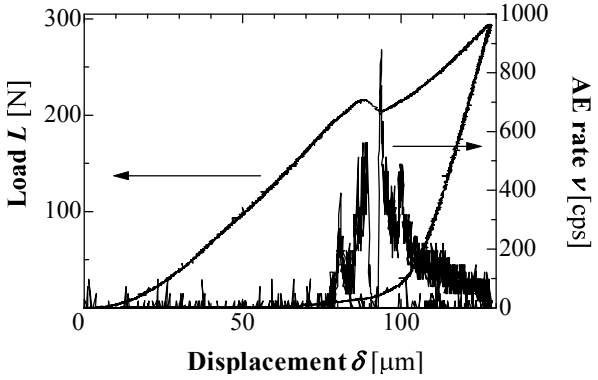

Fig. 6 Relationships between load, AE rate, and displacement of the TBC specimen at 294 N.

Fig. 7 shows the results of calculated Young's modulus on both the TBC and the TC specimen, it means the influence of TC thickness on calculated Young's modulus. On the TC specimen, it is clearly that load dependency of calculated Young's modulus of TC disappeared and Young's modulus of TC was almost constant.

The distribution of the equivalent elastic strain in the specimen around the indenter is shown in Fig. 8 (this corresponds to an indentation load of 49 N). This result indicated that the strained region at lower load is fitted in

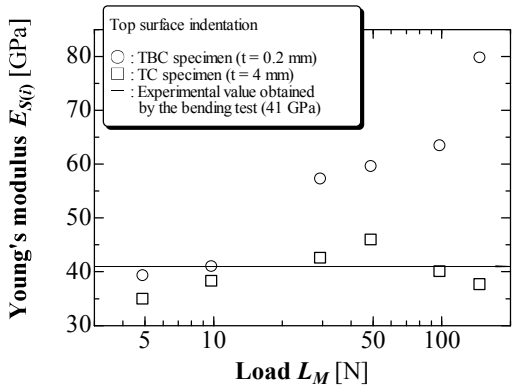

Fig. 7 Influence of TC thickness on calculated Young's modulus of TC.

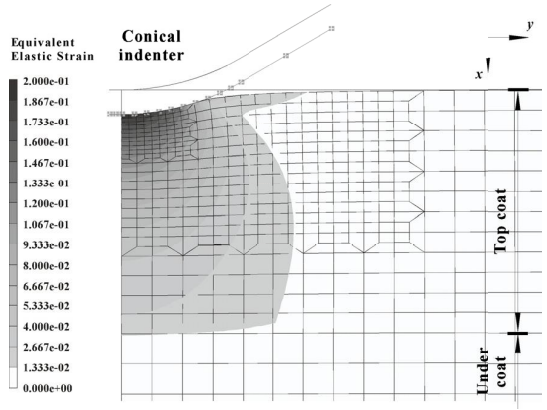

Fig. 8 Distribution of equivalent elastic strain calculated by FEM analysis (20 μm indentation).

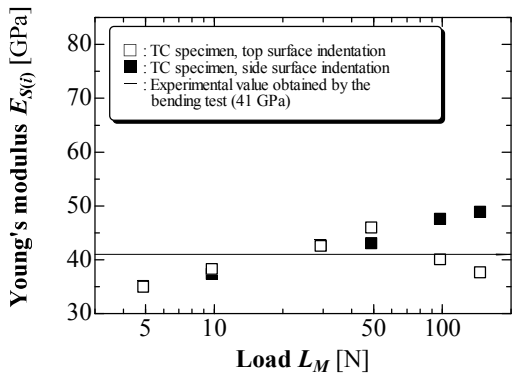

Fig. 9 Influence of indentation direction on calculated Young's modulus of TC.

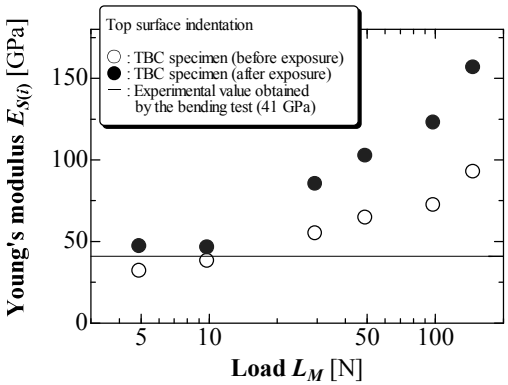

Fig. 11 Influence of long-term high temperature exposure on calculated Young's modulus of TC.

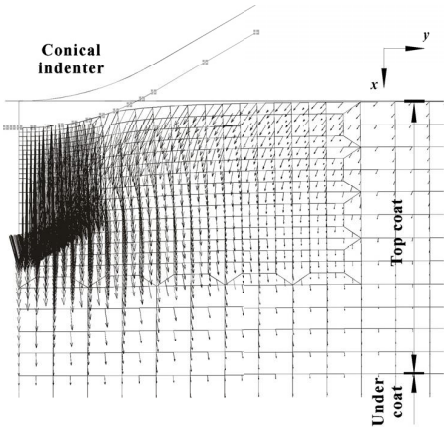

Fig. 10 Distribution of the displacement vector in the specimen around the indenter (20 μm indentation).

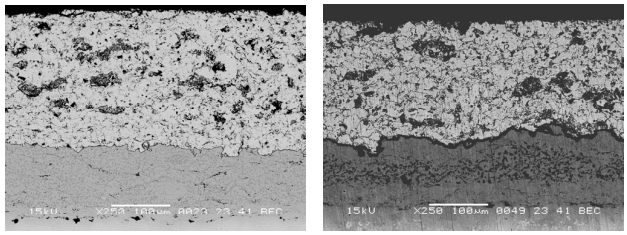

(a) before exposure (b) after exposure

Fig. 12 Cross-sectional observations of TC before / after long-term high temperature exposure (air environment, 900ºC, and 1 year).

Table 2 Results of measured porosity and two kinds of calculated Young's modulus of TC.

	before exposure	after exposure
P [%]	21.4	19.1
$E_{S(p)}$ [GPa]	31.5	38.6
$E_{S(i)}$ [GPa]	35.1	46.9
$(E_{S(i)}-E_{S(p)}/E_{S(i)})\times 100$ [%]	10.3	17.7

TC, but it extend over TC and reached UC in the case of 49 N. Therefore, these results also suggested that the maximum load to calculate TC Young's modulus without any UC effect for this TBC specimen is 9.8 N.

From these results, it is obvious that if the TC thickness is sufficiently large compared to the deformation area caused by a specific indentation load, TC Young's modulus can be calculated without the UC elastic effect. In other words, a pure TC Young's modulus can be obtained by selecting an appropriate indentation load that causes a small deformation area compared with the TC thickness.

3.2. Influence of TC anisotropy

The relationship between the calculated Young's modulus of TC on the side surface indentation of the TC specimen and the indentation load is shown in Fig. 9. For comparison, the calculated TC Young's modulus on the top surface indentation mentioned above is also shown in Fig. 9. From these results, it was obvious that the results of the top surface and the side surface are almost same except for the results of indentation load over 98 N. Therefore, the effect of TC anisotropy on the calculated TC Young's modulus doesn't appear wit h a Young's modulus estimation procedure that uses indentation.

It was reported that TC has anisotropy of mechanical properties from results of the general uniaxial estimation test [12]. However, it was expected that a form of deformation between general uniaxial test and indentation test may be different. Fig. 10 shows the distribution of the displacement vector in the specimen around the indenter caused by indentation of 20 μm depth. It clearly showed that the direction along indentation axis, and also showed that deformation caused by indentation has a three-dimensional area centering on the part of contact between the indenter and specimen.

Therefore, it was supposed that there is difference of anisotropic tendency between general uniaxial test and indentation test. In addition, these results suggest the possibility of misunderstanding for the TC anisotropy estimated by using indentation test.

3.3. Influence of long-term high temperature exposure

Relationship between indentation load and calculated Young's modulus of TC before / after exposure is shown in Fig. 11. After exposure, it is seen that calculated Young's modulus are increased at whole indentation loads with comparison of before exposure.

Fig. 12 (a) and (b) show the cross-sectional images of TC before or after exposure. From these images, two-dimensional porosity and consequently Young's modulus from porosity were calculated. Obtained results were listed in Table 1. From these results, because qualitative tendency between $E_{S(i)}$ and $E_{S(p)}$ corresponded, it was obvious that occurrence of TC densification (decreasing TC porosity) and consequently increasing Young's modulus of TC. In other words, it is able to detect increasing Young's modulus of TC by using indentation test. However, quantitative difference between $E_{S(i)}$ and $E_{S(p)}$ was present. This difference may be caused by such as fitting process from porosity to Young's modulus or image treatment process in the procedure to calculate $E_{S(p)}$. Therefore, it is necessary to review the whole procedure for $E_{S(p)}$.

4. CONCLUSION

We studied Thermal Barrier Coatings applied to gas turbine for electric power stations, in order to estimate top-coat (TC) Young's modulus by using the indentation hardness test. In this study, we discussed influence of load dependency, TC anisotropy and long-term high temperature exposure on calculated TC Young's modulus. The summary of our conclusions is as follows:

(1) From the results of the indentation test with the AE sensor of the TBC specimen, it is confirmed that the reason for the decrease in TC Young's modulus with an increasing indentation load over 147 N is displacement promotion due to TC fracture around the contact area caused by indentation.

(2) From the results of the indentation test on the top surface indentation of the TC specimen, it is confirmed that the reason for the increase in TC Young's modulus with an increasing indentation load below 147 N is the enlargement of the deformation area and the increase of the UC elastic effect.

(3) From the results of the indentation test on the side surface indentation of the TC specimen, it is obviously that the effect of TC anisotropy on the calculated TC Young's modulus doesn't appear by Young's modulus estimation procedure that uses indentation. These results are caused by different form of deformation between general uniaxial test and indentation test, so it may be in danger of misunderstanding for the TC anisotropy estimated by using indentation test.

(4) From the results of the indentation test on the TBC specimens before / after long-term high temperature exposure, it is shown that obviously increasing of calculated Young's modulus at whole indentation loads. This increasing is caused by densification of TC (decreasing of TC porosity) which is confirmed by measurement of TC porosity. Its possibility to detect increasing Young's modulus of TC by using the indentation test was confirmed.

REFERENCES

[1] Y. Itoh, M. Saitoh, M. Takahashi, K. Ikeda, H. Okamoto, K. Takahara, *J. High Temp. Soc.*, vol. 23, no. 1, pp. 37-42, 1997.

[2] M. Ohki, Y. Mutoh, T. Higashiwada, S. Adachi, M. Takahashi, *J. Soc. Mater. Sci. Japan*, vol. 46, no. 8, pp. 939-945, 1997.

[3] M. Ohki, Y. Mutoh, M. Ohara, M. Takahashi, T. Ishibashi, *Quarterly J. Japan Welding Soc.*, vol. 16, no. 3, pp. 395-404, 1998.

[4] T. Ishibashi, M. Ohki, S. Katayama, S. Takagi, *J. Mater. Test. Res. Assoc. JAPAN*, vol. 50, no. 2, pp. 35-42, 2005.

[5] M. Ohki, T. Ishibashi, Y. Miyaji, E. Hatsugai, H. Amano, Y. Nakafuku, *Journal of the JRICu*, vol. 42, no. 1, pp. 188-192, 2003.

[6] J. Malzbender, R. W. Steinbrech, *J. Mater. Res.*, vol. 18, no. 8, pp. 1975-1984, 2003.

[7] H. Amano, T. Ishibashi, S. Sukigara, M. Fujitsuka, H. Sakurai, *J. Mater. Test. Res. Assoc. JAPAN*, vol. 47, no. 3, pp. 26-33, 2002.

[8] H. Amano, T. Ishibashi, M. Ohki, H. Sakurai, M. Fujitsuka, *J. Mater. Test. Res. Assoc. JAPAN*, vol. 48, no. 3, pp. 9-16, 2003.

[9] S. P. Timoshenko, J. N. Goodier, "Theory of Elasticity", *McGraw-Hill*, 1970.

[10] M. Ogami, K. Yamaguchi, H. Nakasa, K. Sano, E. Isono, T. Watanabe, "Acoustic Emission – Bases and Applications", *CORONA*, 1976.

[11] A. C. Fischer-Cripps, "Nanoindentation", *Springer*, 2002.

[12] L. Pawlowski, "The Science and Engineering of Thermal Spray Coatings", *John Wiley & Sons*, 1995.

Author:

Assistant professor Motofumi OHKI, Faculty of Engineering, Niigata University, 8050, Ikarashi 2-no-cho, Nishi-ku, Niigata, 950-2181, Japan, +81-25-262-7926 (Phone & Fax), mohki@eng.niigata-u.ac.jp

Professor Tatsuya ISHIBASHI, Faculty of Engineering, Niigata University, 8050, Ikarashi 2-no-cho, Nishi-ku, Niigata, 950-2181, Japan, +81-25-262-7007 (Phone & Fax), isibasi@eng.niigata-u.ac.jp

Students Jun KINOSHITA and Hiroki UCHIYAMA, Graduate School of Science and Technology, Niigata University, 8050, Ikarashi 2-no-cho, Nishi-ku, Niigata, 950-2181, Japan